

Measurement of the CKM Matrix Element $|V_{ub}|$ with $B \rightarrow \rho e \nu$ Decays

B. Aubert,¹ R. Barate,¹ D. Boutigny,¹ J.-M. Gaillard,¹ A. Hicheur,¹ Y. Karyotakis,¹ J. P. Lees,¹ P. Robbe,¹
V. Tisserand,¹ A. Zghiche,¹ A. Palano,² A. Pompili,² J. C. Chen,³ N. D. Qi,³ G. Rong,³ P. Wang,³ Y. S. Zhu,³
G. Eigen,⁴ I. Ofte,⁴ B. Stugu,⁴ G. S. Abrams,⁵ A. W. Borgland,⁵ A. B. Breon,⁵ D. N. Brown,⁵ J. Button-Shafer,⁵
R. N. Cahn,⁵ E. Charles,⁵ M. S. Gill,⁵ A. V. Gritsan,⁵ Y. Groysman,⁵ R. G. Jacobsen,⁵ R. W. Kadel,⁵ J. Kadyk,⁵
L. T. Kerth,⁵ Yu. G. Kolomensky,⁵ J. F. Kral,⁵ C. LeClerc,⁵ M. E. Levi,⁵ G. Lynch,⁵ L. M. Mir,⁵ P. J. Oddone,⁵
T. J. Orimoto,⁵ M. Pripstein,⁵ N. A. Roe,⁵ A. Romosan,⁵ M. T. Ronan,⁵ V. G. Shelkov,⁵ A. V. Telnov,⁵
W. A. Wenzel,⁵ T. J. Harrison,⁶ C. M. Hawkes,⁶ D. J. Knowles,⁶ S. W. O’Neale,⁶ R. C. Penny,⁶ A. T. Watson,⁶
N. K. Watson,⁶ T. Deppermann,⁷ K. Goetzen,⁷ H. Koch,⁷ B. Lewandowski,⁷ M. Pelizaeus,⁷ K. Peters,⁷
H. Schmuecker,⁷ M. Steinke,⁷ N. R. Barlow,⁸ W. Bhimji,⁸ J. T. Boyd,⁸ N. Chevalier,⁸ P. J. Clark,⁸
W. N. Cottingham,⁸ C. Mackay,⁸ F. F. Wilson,⁸ C. Hearty,⁹ T. S. Mattison,⁹ J. A. McKenna,⁹ D. Thiessen,⁹
S. Jolly,¹⁰ P. Kyberd,¹⁰ A. K. McKemey,¹⁰ V. E. Blinov,¹¹ A. D. Bukin,¹¹ A. R. Buzykaev,¹¹ V. B. Golubev,¹¹
V. N. Ivanchenko,¹¹ A. A. Korol,¹¹ E. A. Kravchenko,¹¹ A. P. Onuchin,¹¹ S. I. Serednyakov,¹¹ Yu. I. Skovpen,¹¹
A. N. Yushkov,¹¹ D. Best,¹² M. Chao,¹² D. Kirkby,¹² A. J. Lankford,¹² M. Mandelkern,¹² S. McMahon,¹²
R. K. Mommsen,¹² D. P. Stoker,¹² C. Buchanan,¹³ H. K. Hadavand,¹⁴ E. J. Hill,¹⁴ D. B. MacFarlane,¹⁴
H. P. Paar,¹⁴ Sh. Rahatlou,¹⁴ G. Raven,¹⁴ U. Schwanke,¹⁴ V. Sharma,¹⁴ J. W. Berryhill,¹⁵ C. Campagnari,¹⁵
B. Dahmes,¹⁵ N. Kuznetsova,¹⁵ S. L. Levy,¹⁵ O. Long,¹⁵ A. Lu,¹⁵ M. A. Mazur,¹⁵ J. D. Richman,¹⁵ W. Verkerke,¹⁵
J. Beringer,¹⁶ A. M. Eisner,¹⁶ M. Grothe,¹⁶ C. A. Heusch,¹⁶ W. S. Lockman,¹⁶ T. Pulliam,¹⁶ T. Schalk,¹⁶
R. E. Schmitz,¹⁶ B. A. Schumm,¹⁶ A. Seiden,¹⁶ M. Turri,¹⁶ W. Walkowiak,¹⁶ D. C. Williams,¹⁶ M. G. Wilson,¹⁶
J. Albert,¹⁷ E. Chen,¹⁷ G. P. Dubois-Felsmann,¹⁷ A. Dvoretzki,¹⁷ D. G. Hitlin,¹⁷ I. Narsky,¹⁷ F. C. Porter,¹⁷
A. Ryd,¹⁷ A. Samuel,¹⁷ S. Yang,¹⁷ S. Jayatilake,¹⁸ G. Mancinelli,¹⁸ B. T. Meadows,¹⁸ M. D. Sokoloff,¹⁸
T. Barillari,¹⁹ F. Blanc,¹⁹ P. Bloom,¹⁹ W. T. Ford,¹⁹ U. Nauenberg,¹⁹ A. Olivas,¹⁹ P. Rankin,¹⁹ J. Roy,¹⁹
J. G. Smith,¹⁹ W. C. van Hoek,¹⁹ L. Zhang,¹⁹ J. L. Harton,²⁰ T. Hu,²⁰ A. Soffer,²⁰ W. H. Toki,²⁰ R. J. Wilson,²⁰
J. Zhang,²⁰ D. Altenburg,²¹ T. Brandt,²¹ J. Brose,²¹ T. Colberg,²¹ M. Dickopp,²¹ R. S. Dubitzky,²¹ A. Hauke,²¹
H. M. Lacker,²¹ E. Maly,²¹ R. Müller-Pfefferkorn,²¹ R. Nogowski,²¹ S. Otto,²¹ K. R. Schubert,²¹ R. Schwierz,²¹
B. Spaan,²¹ L. Wilden,²¹ D. Bernard,²² G. R. Bonneaud,²² F. Brochard,²² J. Cohen-Tanugi,²² S. T’Jampens,²²
Ch. Thiebaux,²² G. Vasileiadis,²² M. Verderi,²² A. Anjomshoaa,²³ R. Bernet,²³ A. Khan,²³ D. Lavin,²³
F. Muheim,²³ S. Playfer,²³ J. E. Swain,²³ J. Tinslay,²³ M. Falbo,²⁴ C. Borean,²⁵ C. Bozzi,²⁵ L. Piemontese,²⁵
A. Sarti,²⁵ E. Treadwell,²⁶ F. Anulli,²⁷ * R. Baldini-Ferrolì,²⁷ A. Calcaterra,²⁷ R. de Sangro,²⁷ D. Falciai,²⁷
G. Finocchiaro,²⁷ P. Patteri,²⁷ I. M. Peruzzi,²⁷ * M. Piccolo,²⁷ A. Zallo,²⁷ S. Bagnasco,²⁸ A. Buzzo,²⁸ R. Contri,²⁸
G. Crosetti,²⁸ M. Lo Vetere,²⁸ M. Macri,²⁸ M. R. Monge,²⁸ S. Passaggio,²⁸ F. C. Pastore,²⁸ C. Patrignani,²⁸
E. Robutti,²⁸ A. Santroni,²⁸ S. Tosi,²⁸ S. Bailey,²⁹ M. Morii,²⁹ G. J. Grenier,³⁰ U. Mallik,³⁰ J. Cochran,³¹
H. B. Crawley,³¹ J. Lamsa,³¹ W. T. Meyer,³¹ S. Prell,³¹ E. I. Rosenberg,³¹ J. Yi,³¹ M. Davier,³² G. Grosdidier,³²
A. Höcker,³² S. Laplace,³² F. Le Diberder,³² V. Lepeltier,³² A. M. Lutz,³² T. C. Petersen,³² S. Plaszczynski,³²
M. H. Schune,³² L. Tantot,³² G. Wormser,³² R. M. Bionta,³³ V. Brigljević,³³ D. J. Lange,³³ K. van Bibber,³³
D. M. Wright,³³ A. J. Bevan,³⁴ J. R. Fry,³⁴ E. Gabathuler,³⁴ R. Gamet,³⁴ M. George,³⁴ M. Kay,³⁴ D. J. Payne,³⁴
R. J. Sloane,³⁴ C. Touramanis,³⁴ M. L. Aspinwall,³⁵ D. A. Bowerman,³⁵ P. D. Dauncey,³⁵ U. Egede,³⁵ I. Eschrich,³⁵
G. W. Morton,³⁵ J. A. Nash,³⁵ P. Sanders,³⁵ G. P. Taylor,³⁵ J. J. Back,³⁶ G. Bellodi,³⁶ P. Dixon,³⁶ P. F. Harrison,³⁶
H. W. Shorthouse,³⁶ P. Strother,³⁶ P. B. Vidal,³⁶ G. Cowan,³⁷ H. U. Flaecher,³⁷ S. George,³⁷ M. G. Green,³⁷
A. Kurup,³⁷ C. E. Marker,³⁷ T. R. McMahon,³⁷ S. Ricciardi,³⁷ F. Salvatore,³⁷ G. Vaitsas,³⁷ M. A. Winter,³⁷
D. Brown,³⁸ C. L. Davis,³⁸ J. Allison,³⁹ R. J. Barlow,³⁹ A. C. Forti,³⁹ P. A. Hart,³⁹ F. Jackson,³⁹ G. D. Lafferty,³⁹
A. J. Lyon,³⁹ N. Savvas,³⁹ J. H. Weatherall,³⁹ J. C. Williams,³⁹ A. Farbin,⁴⁰ A. Jawahery,⁴⁰ V. Lillard,⁴⁰
D. A. Roberts,⁴⁰ G. Blaylock,⁴¹ C. Dallapiccola,⁴¹ K. T. Flood,⁴¹ S. S. Hertzbach,⁴¹ R. Kofler,⁴¹ V. B. Koptchev,⁴¹
T. B. Moore,⁴¹ H. Staengle,⁴¹ S. Willcoq,⁴¹ R. Cowan,⁴² G. Sciolla,⁴² F. Taylor,⁴² R. K. Yamamoto,⁴² M. Milek,⁴³
P. M. Patel,⁴³ F. Palombo,⁴⁴ J. M. Bauer,⁴⁵ L. Cremaldi,⁴⁵ V. Eschenburg,⁴⁵ R. Kroeger,⁴⁵ J. Reidy,⁴⁵
D. A. Sanders,⁴⁵ D. J. Summers,⁴⁵ H. Zhao,⁴⁵ C. Hast,⁴⁶ P. Taras,⁴⁶ H. Nicholson,⁴⁷ C. Cartaro,⁴⁸ N. Cavallo,⁴⁸
G. De Nardo,⁴⁸ F. Fabozzi,⁴⁸ † C. Gatto,⁴⁸ L. Lista,⁴⁸ P. Paolucci,⁴⁸ D. Piccolo,⁴⁸ C. Sciacca,⁴⁸ J. M. LoSecco,⁴⁹

J. R. G. Alsmiller,⁵⁰ T. A. Gabriel,⁵⁰ B. Brau,⁵¹ J. Brau,⁵² R. Frey,⁵² M. Iwasaki,⁵² C. T. Potter,⁵² N. B. Sinev,⁵² D. Strom,⁵² E. Torrence,⁵² F. Colecchia,⁵³ A. Dorigo,⁵³ F. Galeazzi,⁵³ M. Margoni,⁵³ M. Morandin,⁵³ M. Posocco,⁵³ M. Rotondo,⁵³ F. Simonetto,⁵³ R. Stroili,⁵³ G. Tiozzo,⁵³ C. Voci,⁵³ M. Benayoun,⁵⁴ H. Briand,⁵⁴ J. Chauveau,⁵⁴ P. David,⁵⁴ Ch. de la Vaissière,⁵⁴ L. Del Buono,⁵⁴ O. Hamon,⁵⁴ Ph. Leruste,⁵⁴ J. Ocariz,⁵⁴ M. Pivk,⁵⁴ L. Roos,⁵⁴ J. Stark,⁵⁴ P. F. Manfredi,⁵⁵ V. Re,⁵⁵ V. Speziali,⁵⁵ L. Gladney,⁵⁶ Q. H. Guo,⁵⁶ J. Panetta,⁵⁶ C. Angelini,⁵⁷ G. Batignani,⁵⁷ S. Bettarini,⁵⁷ M. Bondioli,⁵⁷ F. Bucci,⁵⁷ G. Calderini,⁵⁷ E. Campagna,⁵⁷ M. Carpinelli,⁵⁷ F. Forti,⁵⁷ M. A. Giorgi,⁵⁷ A. Lusiani,⁵⁷ G. Marchiori,⁵⁷ F. Martinez-Vidal,⁵⁷ M. Morganti,⁵⁷ N. Neri,⁵⁷ E. Paoloni,⁵⁷ M. Rama,⁵⁷ G. Rizzo,⁵⁷ F. Sandrelli,⁵⁷ G. Triggiani,⁵⁷ J. Walsh,⁵⁷ M. Haire,⁵⁸ D. Judd,⁵⁸ K. Paick,⁵⁸ L. Turnbull,⁵⁸ D. E. Wagoner,⁵⁸ N. Danielson,⁵⁹ P. Elmer,⁵⁹ C. Lu,⁵⁹ V. Miftakov,⁵⁹ J. Olsen,⁵⁹ A. J. S. Smith,⁵⁹ A. Tumanov,⁵⁹ E. W. Varnes,⁵⁹ F. Bellini,^{59,60} G. Cavoto,^{59,60} D. del Re,^{14,60} R. Faccini,^{14,60} F. Ferrarotto,⁶⁰ F. Ferroni,⁶⁰ M. Gaspero,⁶⁰ E. Leonardi,⁶⁰ M. A. Mazzoni,⁶⁰ S. Morganti,⁶⁰ G. Piredda,⁶⁰ F. Safai Tehrani,⁶⁰ M. Serra,⁶⁰ C. Voena,⁶⁰ S. Christ,⁶¹ G. Wagner,⁶¹ R. Waldi,⁶¹ T. Adye,⁶² N. De Groot,⁶² B. Franek,⁶² N. I. Geddes,⁶² G. P. Gopal,⁶² E. O. Olaiya,⁶² S. M. Xella,⁶² R. Aleksan,⁶³ S. Emery,⁶³ A. Gaidot,⁶³ P.-F. Giraud,⁶³ G. Hamel de Monchenault,⁶³ W. Kozanecki,⁶³ M. Langer,⁶³ G. W. London,⁶³ B. Mayer,⁶³ G. Schott,⁶³ B. Serfass,⁶³ G. Vasseur,⁶³ Ch. Yeche,⁶³ M. Zito,⁶³ M. V. Purohit,⁶⁴ A. W. Weidemann,⁶⁴ F. X. Yumiceva,⁶⁴ K. Abe,⁶⁵ D. Aston,⁶⁵ R. Bartoldus,⁶⁵ N. Berger,⁶⁵ A. M. Boyarski,⁶⁵ O. L. Buchmueller,⁶⁵ M. R. Convery,⁶⁵ D. P. Coupal,⁶⁵ D. Dong,⁶⁵ J. Dorfan,⁶⁵ W. Dunwoodie,⁶⁵ R. C. Field,⁶⁵ T. Glanzman,⁶⁵ S. J. Gowdy,⁶⁵ E. Grauges-Pous,⁶⁵ T. Hadig,⁶⁵ V. Halyo,⁶⁵ T. Himel,⁶⁵ T. Hryn'ova,⁶⁵ M. E. Huffer,⁶⁵ W. R. Innes,⁶⁵ C. P. Jessop,⁶⁵ M. H. Kelsey,⁶⁵ P. Kim,⁶⁵ M. L. Kocian,⁶⁵ U. Langenegger,⁶⁵ D. W. G. S. Leith,⁶⁵ S. Luitz,⁶⁵ V. Luth,⁶⁵ H. L. Lynch,⁶⁵ H. Marsiske,⁶⁵ S. Menke,⁶⁵ R. Messner,⁶⁵ D. R. Muller,⁶⁵ C. P. O'Grady,⁶⁵ V. E. Ozcan,⁶⁵ A. Perazzo,⁶⁵ M. Perl,⁶⁵ S. Petrak,⁶⁵ B. N. Ratcliff,⁶⁵ S. H. Robertson,⁶⁵ A. Roodman,⁶⁵ A. A. Salnikov,⁶⁵ T. Schietinger,⁶⁵ R. H. Schindler,⁶⁵ J. Schwiening,⁶⁵ G. Simi,⁶⁵ A. Snyder,⁶⁵ A. Soha,⁶⁵ J. Stelzer,⁶⁵ D. Su,⁶⁵ M. K. Sullivan,⁶⁵ H. A. Tanaka,⁶⁵ J. Va'vra,⁶⁵ S. R. Wagner,⁶⁵ M. Weaver,⁶⁵ A. J. R. Weinstein,⁶⁵ W. J. Wisniewski,⁶⁵ D. H. Wright,⁶⁵ C. C. Young,⁶⁵ P. R. Burchat,⁶⁶ C. H. Cheng,⁶⁶ T. I. Meyer,⁶⁶ C. Roat,⁶⁶ W. Bugg,⁶⁷ M. Krishnamurthy,⁶⁷ S. M. Spanier,⁶⁷ J. M. Izen,⁶⁸ I. Kitayama,⁶⁸ X. C. Lou,⁶⁸ F. Bianchi,⁶⁹ M. Bona,⁶⁹ D. Gamba,⁶⁹ L. Bosisio,⁷⁰ G. Della Ricca,⁷⁰ S. Dittongo,⁷⁰ L. Lanceri,⁷⁰ P. Poropat,⁷⁰ L. Vitale,⁷⁰ G. Vuagnin,⁷⁰ R. Henderson,⁷¹ R. S. Panvini,⁷² Sw. Banerjee,⁷³ C. M. Brown,⁷³ D. Fortin,⁷³ P. D. Jackson,⁷³ R. Kowalewski,⁷³ J. M. Roney,⁷³ H. R. Band,⁷⁴ S. Dasu,⁷⁴ M. Datta,⁷⁴ A. M. Eichenbaum,⁷⁴ H. Hu,⁷⁴ J. R. Johnson,⁷⁴ R. Liu,⁷⁴ F. Di Lodovico,⁷⁴ A. K. Mohapatra,⁷⁴ Y. Pan,⁷⁴ R. Prepost,⁷⁴ S. J. Sekula,⁷⁴ J. H. von Wimmersperg-Toeller,⁷⁴ J. Wu,⁷⁴ S. L. Wu,⁷⁴ Z. Yu,⁷⁴ and H. Neal⁷⁵

(The BABAR Collaboration)

¹Laboratoire de Physique des Particules, F-74941 Annecy-le-Vieux, France

²Università di Bari, Dipartimento di Fisica and INFN, I-70126 Bari, Italy

³Institute of High Energy Physics, Beijing 100039, China

⁴University of Bergen, Inst. of Physics, N-5007 Bergen, Norway

⁵Lawrence Berkeley National Laboratory and University of California, Berkeley, CA 94720, USA

⁶University of Birmingham, Birmingham, B15 2TT, United Kingdom

⁷Ruhr Universität Bochum, Institut für Experimentalphysik 1, D-44780 Bochum, Germany

⁸University of Bristol, Bristol BS8 1TL, United Kingdom

⁹University of British Columbia, Vancouver, BC, Canada V6T 1Z1

¹⁰Brunel University, Uxbridge, Middlesex UB8 3PH, United Kingdom

¹¹Budker Institute of Nuclear Physics, Novosibirsk 630090, Russia

¹²University of California at Irvine, Irvine, CA 92697, USA

¹³University of California at Los Angeles, Los Angeles, CA 90024, USA

¹⁴University of California at San Diego, La Jolla, CA 92093, USA

¹⁵University of California at Santa Barbara, Santa Barbara, CA 93106, USA

¹⁶University of California at Santa Cruz, Institute for Particle Physics, Santa Cruz, CA 95064, USA

¹⁷California Institute of Technology, Pasadena, CA 91125, USA

¹⁸University of Cincinnati, Cincinnati, OH 45221, USA

¹⁹University of Colorado, Boulder, CO 80309, USA

²⁰Colorado State University, Fort Collins, CO 80523, USA

²¹Technische Universität Dresden, Institut für Kern- und Teilchenphysik, D-01062 Dresden, Germany

²²Ecole Polytechnique, LLR, F-91128 Palaiseau, France

²³University of Edinburgh, Edinburgh EH9 3JZ, United Kingdom

²⁴Elon University, Elon University, NC 27244-2010, USA

²⁵Università di Ferrara, Dipartimento di Fisica and INFN, I-44100 Ferrara, Italy

- ²⁶Florida A&M University, Tallahassee, FL 32307, USA
²⁷Laboratori Nazionali di Frascati dell'INFN, I-00044 Frascati, Italy
²⁸Università di Genova, Dipartimento di Fisica and INFN, I-16146 Genova, Italy
²⁹Harvard University, Cambridge, MA 02138, USA
³⁰University of Iowa, Iowa City, IA 52242, USA
³¹Iowa State University, Ames, IA 50011-3160, USA
³²Laboratoire de l'Accélérateur Linéaire, F-91898 Orsay, France
³³Lawrence Livermore National Laboratory, Livermore, CA 94550, USA
³⁴University of Liverpool, Liverpool L69 3BX, United Kingdom
³⁵University of London, Imperial College, London, SW7 2BW, United Kingdom
³⁶Queen Mary, University of London, E1 4NS, United Kingdom
³⁷University of London, Royal Holloway and Bedford New College, Egham, Surrey TW20 0EX, United Kingdom
³⁸University of Louisville, Louisville, KY 40292, USA
³⁹University of Manchester, Manchester M13 9PL, United Kingdom
⁴⁰University of Maryland, College Park, MD 20742, USA
⁴¹University of Massachusetts, Amherst, MA 01003, USA
⁴²Massachusetts Institute of Technology, Laboratory for Nuclear Science, Cambridge, MA 02139, USA
⁴³McGill University, Montréal, QC, Canada H3A 2T8
⁴⁴Università di Milano, Dipartimento di Fisica and INFN, I-20133 Milano, Italy
⁴⁵University of Mississippi, University, MS 38677, USA
⁴⁶Université de Montréal, Laboratoire René J. A. Lévesque, Montréal, QC, Canada H3C 3J7
⁴⁷Mount Holyoke College, South Hadley, MA 01075, USA
⁴⁸Università di Napoli Federico II, Dipartimento di Scienze Fisiche and INFN, I-80126, Napoli, Italy
⁴⁹University of Notre Dame, Notre Dame, IN 46556, USA
⁵⁰Oak Ridge National Laboratory, Oak Ridge, TN 37831, USA
⁵¹Ohio State Univ., 174 W.18th Ave., Columbus, OH 43210
⁵²University of Oregon, Eugene, OR 97403, USA
⁵³Università di Padova, Dipartimento di Fisica and INFN, I-35131 Padova, Italy
⁵⁴Universités Paris VI et VII, Lab de Physique Nucléaire H. E., F-75252 Paris, France
⁵⁵Università di Pavia, Dipartimento di Elettronica and INFN, I-27100 Pavia, Italy
⁵⁶University of Pennsylvania, Philadelphia, PA 19104, USA
⁵⁷Università di Pisa, Scuola Normale Superiore and INFN, I-56010 Pisa, Italy
⁵⁸Prairie View A&M University, Prairie View, TX 77446, USA
⁵⁹Princeton University, Princeton, NJ 08544, USA
⁶⁰Università di Roma La Sapienza, Dipartimento di Fisica and INFN, I-00185 Roma, Italy
⁶¹Universität Rostock, D-18051 Rostock, Germany
⁶²Rutherford Appleton Laboratory, Chilton, Didcot, Oxon, OX11 0QX, United Kingdom
⁶³DAPNIA, Commissariat à l'Energie Atomique/Saclay, F-91191 Gif-sur-Yvette, France
⁶⁴University of South Carolina, Columbia, SC 29208, USA
⁶⁵Stanford Linear Accelerator Center, Stanford, CA 94309, USA
⁶⁶Stanford University, Stanford, CA 94305-4060, USA
⁶⁷University of Tennessee, Knoxville, TN 37996, USA
⁶⁸University of Texas at Dallas, Richardson, TX 75083, USA
⁶⁹Università di Torino, Dipartimento di Fisica Sperimentale and INFN, I-10125 Torino, Italy
⁷⁰Università di Trieste, Dipartimento di Fisica and INFN, I-34127 Trieste, Italy
⁷¹TRIUMF, Vancouver, BC, Canada V6T 2A3
⁷²Vanderbilt University, Nashville, TN 37235, USA
⁷³University of Victoria, Victoria, BC, Canada V8W 3P6
⁷⁴University of Wisconsin, Madison, WI 53706, USA
⁷⁵Yale University, New Haven, CT 06511, USA

(Dated: October 18, 2018)

We present a measurement of the branching fraction for the rare decays $B \rightarrow pe\nu$ and extract a value for the magnitude of V_{ub} , one of the smallest elements of the Cabibbo-Kobayashi-Maskawa quark-mixing matrix. The results are given for five different calculations of form factors used to parametrize the hadronic current in semileptonic decays. Using a sample of 55 million $B\bar{B}$ meson pairs recorded with the BABAR detector at the PEP-II e^+e^- storage ring, we obtain $\mathcal{B}(B^0 \rightarrow \rho^- e^+ \nu) = (3.29 \pm 0.42 \pm 0.47 \pm 0.60) \times 10^{-4}$ and $|V_{ub}| = (3.64 \pm 0.22 \pm 0.25_{-0.56}^{+0.39}) \times 10^{-3}$, where the uncertainties are statistical, systematic, and theoretical, respectively.

PACS numbers: 13.20.He, 12.15.Hh, 14.40.Nd

Exclusive $b \rightarrow ul\nu$ decays can be used to determine $|V_{ub}|$, one of the smallest and least well-determined ele-

ments of the Cabibbo-Kobayashi-Maskawa quark-mixing matrix. The modes $B \rightarrow \rho e \nu$ have a comparatively large branching fraction, and a high fraction of events is found at large electron momenta. We determine both the branching fraction $\mathcal{B}(B \rightarrow \rho e \nu)$ and $|V_{ub}|$ using form factors, which describe the hadronic current in the decay, to extrapolate the decay rates to the full range of lepton energies and to normalize \mathcal{B} to $|V_{ub}|$. Five different form-factor calculations are used, as given in Table I.

The data in this analysis were collected with the *BABAR* detector [6] at the PEP-II [7] asymmetric-energy e^+e^- storage ring. The integrated luminosity of the sample recorded on the $\Upsilon(4S)$ resonance in years 2000 and 2001 (“on-resonance”) is 50.5 fb^{-1} , corresponding to 55.2 million $B\bar{B}$ meson pairs. An additional 8.7 fb^{-1} of data were taken 40 MeV below the resonance (“off-resonance”). *BABAR* is a detector optimized for the asymmetric beam configuration at PEP-II. Charged-particle momenta are measured in a tracking system consisting of a 5-layer, double-sided silicon vertex tracker (SVT) and a 40-layer drift chamber (DCH) filled with a mixture of helium and isobutane, both operating in a 1.5-T superconducting solenoid. The electromagnetic calorimeter (EMC) consists of 6580 CsI(Tl) crystals arranged in barrel and forward endcap subdetectors. Particle identification is performed by combining information from ionization measurements in the SVT and DCH, energy deposits in the EMC, and the angle and number of Cherenkov photons measured by the DIRC (detector of internally reflected Cherenkov light).

We select decays in the modes $B^+ \rightarrow \rho^0 e^+ \nu$, $B^0 \rightarrow \rho^- e^+ \nu$, $B^+ \rightarrow \omega e^+ \nu$, $B^+ \rightarrow \pi^0 e^+ \nu$, and $B^0 \rightarrow \pi^- e^+ \nu$, with $\rho^0 \rightarrow \pi^+ \pi^-$, $\rho^- \rightarrow \pi^0 \pi^-$, and $\omega \rightarrow \pi^0 \pi^+ \pi^-$. The inclusion of charge conjugate decays is implied throughout. The analysis is optimized for $B \rightarrow \rho e \nu$ decays, similar to that in Ref. [8]. Each signal event is sometimes reconstructed in one of the four other modes; the π and ω modes are included in order to estimate this crossfeed into the ρ modes. Throughout this paper, all variables are expressed in the $\Upsilon(4S)$ center-of-mass frame, except if stated otherwise. Two electron-energy regions are considered: $2.0 \leq E_e < 2.3 \text{ GeV}$ (*low- E_e*) and $2.3 \leq E_e < 2.7 \text{ GeV}$ (*high- E_e*). A large background to $b \rightarrow ue\nu$ decays comes from the more copious $b \rightarrow ce\nu$ decays. This background is kinematically suppressed in the high- E_e region and dominates in the low- E_e region. The low- E_e region provides the background normalization in the high- E_e region. The largest background in the high- E_e region is continuum $e^+e^- \rightarrow q\bar{q}$ events. The off-resonance data are used to estimate its size.

Hadronic events are selected based on track and photon multiplicity and event topology. We use tracks originating from the interaction point with at least 12 hits in the DCH and a transverse momentum greater than 0.1 GeV/ c . Signals in the EMC with $E_{lab} > 30 \text{ MeV}$ that are not associated with any track are considered as

TABLE I: Form-factor calculations used in the determination of $\mathcal{B}(B \rightarrow \rho e \nu)$ and $|V_{ub}|$, and predicted normalizations $\bar{\Gamma}_{\text{th}}$ (as defined later in Eq. 3).

Form factors	$\bar{\Gamma}_{\text{th}}$ (ps^{-1})	Error (%)	Reference
ISGW2	14.2	± 50	[1]
Beyer/Melikhov	16.0	± 15	[2]
UKQCD	16.5	+21, -14	[3]
LCSR	16.9	± 32	[4]
Ligeti/Wise	19.4	± 29	[5]

photons if the lateral moment of the shower energy distribution [9] is smaller than 0.8. We select events with at least five tracks, or with at least four tracks and at least five photons. We require the ratio H_2/H_0 of Fox-Wolfram moments [10] to be less than 0.4. This requirement keeps 85% of the $\rho e \nu$ signal; it rejects 55% of the non- $B\bar{B}$ events.

Electrons are identified with a likelihood estimator using information from the DCH, EMC, and DIRC subdetectors [11]. The selection efficiency is around 90%, with a pion misidentification rate of less than 0.1%. We reject electrons from J/ψ decays and from photon conversions.

Charged pion candidates are tracks not identified as kaons with high confidence based on DIRC and dE/dx measurements. A π^0 is reconstructed from photon pairs with an invariant mass $120 < M_{\gamma\gamma} < 145 \text{ MeV}/c^2$.

To reconstruct ρ^0 mesons, we combine two oppositely-charged pions, and for ρ^\pm a pion track and a π^0 . To suppress combinatorial background we require that the pion with the higher momentum satisfies $p_\pi > 400 \text{ MeV}/c$ and the other pion $p_\pi > 200 \text{ MeV}/c$. For the ω , we combine two oppositely-charged pions with a π^0 . To suppress combinatorial background we require $p_\pi > 100 \text{ MeV}/c$ for each pion. In the mode $B \rightarrow \pi e \nu$ we require $p_\pi > 200 \text{ MeV}/c$.

The missing momentum in the event is given by

$$\vec{p}_{\text{miss}} = - \sum_{\text{tracks}} \vec{p}_i - \sum_{\text{photons}} \vec{p}_i, \quad (1)$$

where the sums are over all accepted tracks and photons. We require $|\cos \theta_{\text{miss}}| < 0.9$, where θ_{miss} is the angle between \vec{p}_{miss} and the beam axis. This rejects events with missing high-momentum particles close to the beam axis. We also compare the direction of \vec{p}_{miss} with that of the neutrino inferred from $\vec{p}_\nu = \vec{p}_B - \vec{p}_Y$, where Y is the $\rho + e$, $\omega + e$, or $\pi + e$ system. The latter is known to within an azimuthal ambiguity about the B direction since only the magnitude of \vec{p}_B is known. We use the smallest possible angle $\Delta\theta_{\text{min}}$ between the two directions and require $\cos \Delta\theta_{\text{min}} > 0.8$. Using the constraints $E_B = E_{\text{beam}}$ and $p_\nu^2 = (p_B - p_Y)^2 = 0$, the angle between the

B meson and the Y system is

$$\cos \theta_{BY} = \frac{2E_B E_Y - (M_B^2 + M_Y^2)c^4}{2|\vec{p}_B||\vec{p}_Y|c^2}. \quad (2)$$

Signal events fulfill $|\cos \theta_{BY}| \leq 1$; allowing for detector resolution we require $|\cos \theta_{BY}| < 1.1$. After all other selection criteria, this requirement rejects more than 60% of the $b \rightarrow ce\nu$ and approximately 68% of the remaining continuum backgrounds, it retains 98% of the signal.

To further reduce the continuum background, we use a neural net with 14 event-shape variables: the sum of track and photon energies in nine cones centered on the lepton-momentum; the angle θ_{thrust} between the thrust axis of the Y system and the thrust axis of the rest of the event (the thrust axis is defined to be the direction that maximizes the sum of the longitudinal momenta of all particles); the angle $\theta_{\text{thrust},Y}$ between the thrust of the Y system and the beam axis; the angle $\theta_{\text{lept,rest}}$ between the direction of the lepton and the direction of the total momentum of all tracks except the Y system; the momentum of the track with the smallest opening angle with respect to the electron; $\sum_i \vec{p}_i \cdot \vec{n}_e / \sum_i |\vec{p}_i|$, where \vec{n}_e is the direction of the electron and \vec{p}_i are the momenta of all tracks except the electron. After all other selection criteria, the neural net condition removes more than 90% of the continuum events in the high- E_e region, while retaining approximately 60% of the signal events in each signal mode.

After all selections, there remain on average 3.4 candidates per event. We choose the one with a total momentum $|\vec{p}_Y + \vec{p}_{\text{miss}}|$ closest to the B -meson momentum $|\vec{p}_B|$. The probability of making the right choice for the signal modes is approximately 85%.

The total efficiency in the high- E_e region is 12.0% (9.5%) for the mode $B^+ \rightarrow \rho^0 e^+ \nu$ ($B^0 \rightarrow \rho^- e^+ \nu$) in the ISGW2 model; it is 4.2% (3.3%), when relating the accepted events in the high- E_e region to events with all electron energies.

We perform a binned maximum-likelihood fit to the two-dimensional distribution $(M_{\pi\pi(\pi)}, \Delta E)$, where $M_{\pi\pi(\pi)}$ is the invariant mass of the ρ (ω) meson and ΔE is the difference between the reconstructed and the expected B -meson energy, $\Delta E \equiv E_{\text{hadron}} + E_e + |\vec{p}_{\text{miss}}|c - E_{\text{beam}}$. The fit is performed simultaneously for the five signal modes in the two E_e ranges. For the $B \rightarrow \rho e \nu$ modes, the data are divided into 10×10 bins over the $(M_{\pi\pi}, \Delta E)$ region $0.25 \leq M_{\pi\pi} \leq 2.00$ GeV/ c^2 and $|\Delta E| \leq 2$ GeV. For the ω channel, we use five bins in the range $702 \leq M_{\pi\pi} \leq 862$ MeV/ c^2 and ten bins in $|\Delta E| \leq 2$ GeV. For the modes $B \rightarrow \pi e \nu$, only ΔE is used as a fit variable, also with ten bins.

In the fit, the likelihood is calculated as product of probability distributions for each of the five signal modes, for other $b \rightarrow ue\nu$ decays, for $b \rightarrow ce\nu$ decays, for continuum events, and for a small contribution due to misidentified electrons. Shapes and normalizations of the con-

tinuum background and misidentified electrons are extracted from the data. For all other contributions, Monte Carlo (MC) simulation provides the shapes of the distributions. The decays $B \rightarrow D^{(*)}e\nu$ are simulated using a model based on heavy quark effective theory [12]. The modes $B \rightarrow D^{(*)}\pi e\nu$ are simulated according to the Goity-Roberts model [13]. The resonances $b \rightarrow ue\nu$ heavier than ρ and ω are implemented according to the ISGW2 model [1]. Non-resonant $b \rightarrow ue\nu$ modes are described by the model of Fazio and Neubert [14].

The fit has nine free parameters: $\mathcal{B}(B^0 \rightarrow \rho^- e^+ \nu)$, $\mathcal{B}(B^0 \rightarrow \pi^- e^+ \nu)$, the normalization of the $b \rightarrow ue\nu$ background in the two electron-energy ranges (two parameters), and the normalization of the $b \rightarrow ce\nu$ background (five parameters, one for each mode). The rates of the ρ^0 , ω , and π^0 channel are constrained by the isospin and quark model relations $\Gamma(B^0 \rightarrow \rho^- e^+ \nu) = 2\Gamma(B^+ \rightarrow \rho^0 e^+ \nu)$, $\Gamma(B^+ \rightarrow \rho^0 e^+ \nu) = \Gamma(B^+ \rightarrow \omega e^+ \nu)$, and $\Gamma(B^0 \rightarrow \pi^- e^+ \nu) = 2\Gamma(B^+ \rightarrow \pi^0 e^+ \nu)$. The maximum-likelihood fit takes into account the statistical uncertainties in the on- and off-resonance data and in the probability distributions extracted from MC simulations [15].

Projections of the data and fit results for $B^0 \rightarrow \rho^- e^+ \nu$ are shown in Fig. 1 for the ISGW2 model. A continuum-background contribution of 917 ± 73 events in high- E_e and 1928 ± 106 in low- E_e has been subtracted. Good agreement between data and the fit result is seen in each of these figures. The fits for the other form-factor calculations show the same level of agreement. The fit quality has been checked with a χ^2 test, where bins in sparsely populated regions have been combined before the χ^2 calculation. We obtain $\chi^2 = 91$ for 93 degrees of freedom for ISGW2, and similarly good fit quality for the other form-factor calculations. The signal yields extracted from the maximum-likelihood fit in the high- E_e region are 321 ± 40 $B^+ \rightarrow \rho^0 e^+ \nu$ events and 505 ± 63 $B^0 \rightarrow \rho^- e^+ \nu$ events. The resulting branching fractions $\mathcal{B}(B^0 \rightarrow \rho^- e^+ \nu)$ are shown in Fig. 2. The five fit parameters describing the $b \rightarrow ce\nu$ backgrounds agree with the known branching fractions [16] for $B \rightarrow De\nu$, $B \rightarrow D^*e\nu$, and $B \rightarrow D^{(*)}(\pi)e\nu$ within $\pm 9\%$ on average. The two parameters describing the size of the background from other $b \rightarrow ue\nu$ decays agree within 1.5σ with the predictions of the MC simulation. The fit result for the π modes is $\mathcal{B}(B^0 \rightarrow \pi^- e^+ \nu) = (1.86 \pm 0.56_{\text{stat.}}) \times 10^{-4}$ for the ISGW2 model.

A summary of all considered systematic uncertainties on $\mathcal{B}(B \rightarrow \rho e \nu)$ is given in Table II. The total systematic uncertainty is the quadratic sum of all individual ones. Note that the statistical uncertainties in Fig. 2 already include the statistical uncertainty in the MC predictions. The largest single contribution to the systematic error arises from the uncertainty in the shape of the $b \rightarrow ue\nu$ background from events other than the signal modes. The fraction of $b \rightarrow ue\nu$ background events that are non-resonant is varied from 0 to $2/3$ to estimate this

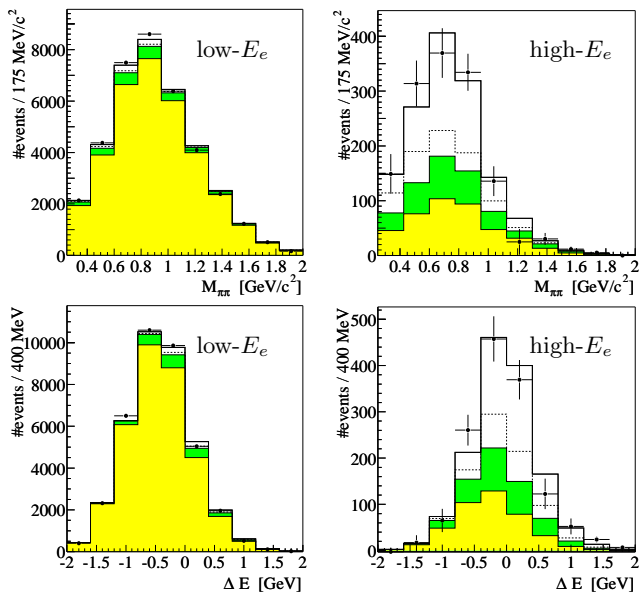


FIG. 1: Continuum-subtracted data distributions (points with error bars) and fit projections (histograms) for $M_{\pi\pi}$ (top plots) and ΔE (bottom plots) for the $B^0 \rightarrow \rho^- e^+ \nu$ channel in the low- E_e (left plots) and high- E_e regions (right plots). The fit results are shown for the ISGW2 model. The histograms correspond to the true and crossfeed components of the signal (open histogram, above and below the dashed line, respectively), the background from other $b \rightarrow ue\nu$ decays (dark shaded region), and $b \rightarrow ce\nu$ and other backgrounds (light shaded region).

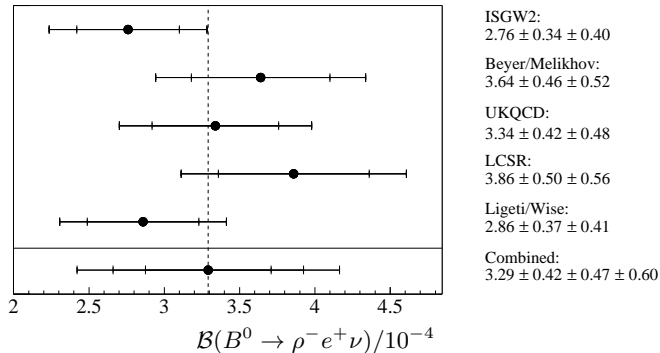


FIG. 2: The $B^0 \rightarrow \rho^- e^+ \nu$ branching fraction results using five different form-factors calculations. The uncertainties shown are statistical, systematic, and (for the combined result) theoretical, successively added in quadrature. The combined result is the average of the five form-factor results.

uncertainty. The composition of the resonant component of other $b \rightarrow ue\nu$ decays has been varied by changing the branching fractions for individual resonances by $\pm 50\%$, while keeping the total rate constant. Variations in the $b \rightarrow ce\nu$ composition contribute much less to the total systematic error than variations in the $b \rightarrow ue\nu$ component. Possible violations of the isospin and quark model

TABLE II: Summary of all contributions to the systematic uncertainty on the branching fraction $\mathcal{B}(B \rightarrow \rho e \nu)$.

Contribution	$\delta\mathcal{B}_\rho/\mathcal{B}_\rho$ (%)
Tracking efficiency	± 5
Tracking resolution	± 1
π^0 efficiency	± 5
π^0 energy scale	± 3
$b \rightarrow ce\nu$ background composition	+1.4, -1.7
Resonant $b \rightarrow ue\nu$ background composition	+6, -4
Non-resonant $b \rightarrow ue\nu$ background	± 9
B lifetime	± 1
Number of $B\bar{B}$ pairs	± 1.6
Misidentified electrons	$< \pm 1$
Electron efficiency	± 2
$\mathcal{B}(\Upsilon(4S) \rightarrow B^+ B^-)/\mathcal{B}(\Upsilon(4S) \rightarrow B^0 \bar{B}^0)$	$< \pm 1$
Isospin and quark model symmetries	$< \pm 1$
Fit method	+4, -6
Total systematic uncertainty	± 14.4

constraints are discussed in Refs. [17] and [18]. Their contribution to the systematic error is determined by allowing a $\pm 3\%$ violation. Several fits were performed: fitting without the ω mode, without the π mode (fixing $\mathcal{B}(B \rightarrow \pi e \nu)$ [16]), without the low- E_e region, and with different binning. We assign a systematic uncertainty for the fit method as half the largest resulting changes of the fit result. We have also varied the most important selection requirements and find that the changes in $\mathcal{B}(B \rightarrow \rho e \nu)$ are consistent with statistical variations as determined by a MC simulation.

A value of $|V_{ub}|$ is determined by the relation

$$|V_{ub}| = \sqrt{\mathcal{B}(B^0 \rightarrow \rho^- e^+ \nu)/(\tilde{\Gamma}_{\text{th}}\tau_{B^0})}, \quad (3)$$

where $\tilde{\Gamma}_{\text{th}}$ is the predicted form-factor normalization as given in Table I. The branching fractions are used separately for each form-factor calculation, as shown in Fig. 2. We use $\tau_{B^0} = 1.542 \pm 0.016$ ps [16] for the B^0 lifetime. The results for $|V_{ub}|$ are shown in Fig. 3. The combined result has been obtained as weighted average of the five form-factor results, where the weight is obtained from the theoretical uncertainty of each. The theoretical uncertainty on the combined result is estimated to be half of the full spread of all theoretical uncertainties.

In conclusion, we have measured the branching fraction $\mathcal{B}(B^0 \rightarrow \rho^- e^+ \nu) = (3.29 \pm 0.42 \pm 0.47 \pm 0.60) \times 10^{-4}$ using isospin constraints and extrapolating to all electron energies according to five different form-factor calculations. The errors given are statistical, systematic, and theoretical, in the order shown. The value of $|V_{ub}|$ determined by the same form-factor calculations is $|V_{ub}| = (3.64 \pm 0.22 \pm 0.25^{+0.39}_{-0.56}) \times 10^{-3}$. Our results are slightly higher (22% for \mathcal{B} and 13% for $|V_{ub}|$) than a previous $B \rightarrow \rho e \nu$ result from CLEO [8], but agree within statistical errors.

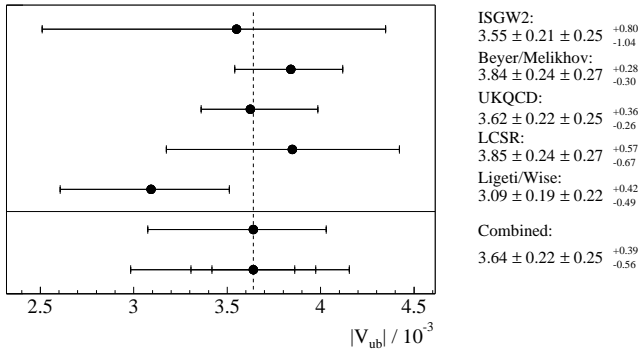


FIG. 3: $|V_{ub}|$ determined using five different form-factor calculations. Only theoretical error bars are shown. The combined result is also shown at the bottom with statistical, systematic, and theoretical uncertainties successively added in quadrature. The combined result is the weighted average of the five form-factor results, where we have used only the theoretical uncertainties to calculate the weights.

We are grateful for the excellent luminosity and machine conditions provided by our PEP-II colleagues, and for the substantial dedicated effort from the computing organizations that support *BABAR*. The collaborating institutions wish to thank SLAC for its support and kind hospitality. This work is supported by DOE and NSF (USA), NSERC (Canada), IHEP (China), CEA and CNRS-IN2P3 (France), BMBF and DFG (Germany), INFN (Italy), NFR (Norway), MIST (Russia), and PPARC (United Kingdom). Individuals have received support from the A. P. Sloan Foundation, Research Corporation, and Alexander von Humboldt Foun-

ation.

* Also with Università di Perugia, Perugia, Italy

† Also with Università della Basilicata, Potenza, Italy

- [1] D. Scora and N. Isgur, Phys. Rev. **D52**, 2783 (1995).
- [2] M. Beyer and D. Melikhov, Phys. Lett. **B436**, 344 (1998).
- [3] L. Del Debbio *et al.*, Phys. Lett. **B416**, 392 (1998).
- [4] P. Ball and V.M. Braun, Phys. Rev. **D58**, 094016 (1998).
- [5] Z. Ligeti and M.B. Wise, Phys. Rev. **D53**, 4937 (1996).
- [6] *BABAR* Collaboration, B. Aubert *et al.*, Nucl. Instr. and Meth. **A479**, 1 (2002).
- [7] “PEP-II Conceptual Design Report”, SLAC-PUB-418, LBL-5379 (1993).
- [8] CLEO Collaboration, B.H. Behrens *et al.*, Phys. Rev. **D61**, 052001 (2000).
- [9] A. Drescher *et al.*, Nucl. Instr. and Meth. **A237**, 464 (1985).
- [10] G.C. Fox and S. Wolfram, Nucl. Phys. **B149**, 413 (1979).
- [11] *BABAR* Collaboration, B. Aubert *et al.*, hep-ex/0208018, SLAC-PUB-9306.
- [12] I.I. Bigi *et al.*, Annu. Rev. Nucl. Part. Sci. **47**, 591 (1997).
- [13] J.L. Goity and W. Roberts, Phys. Rev. **D51**, 3459 (1995).
- [14] F. Fazio and M. Neubert, Journal of High Energy Physics **9906**, 017 (1999).
- [15] R.J. Barlow and C. Beeston, Comp. Phys. Comm. **77**, 219 (1993).
- [16] Particle Data Group, K. Hagiwara *et al.*, Phys. Rev. **D66**, 10001 (2002).
- [17] J.L. Diaz-Cruz *et al.*, Phys. Rev. **D54**, 2388 (1996).
- [18] D.J. Lange, Ph.D. Thesis, University of California, Santa Barbara (1999).
- [19] J.P. Alexander *et al.*, Phys. Rev. Lett. **77**, 5000 (1996).